Time of Emergence of compound events: contribution of univariate and dependence properties

Bastien François[1] and Mathieu Vrac[1]

[1]Laboratoire des Sciences du Climat et l'Environnement (LSCE-IPSL) CNRS/CEA/UVSQ, UMR8212, Université Paris-Saclay, Gif-sur-Yvette, France

Correspondence: B. François (bastien.francois@lsce.ipsl.fr)

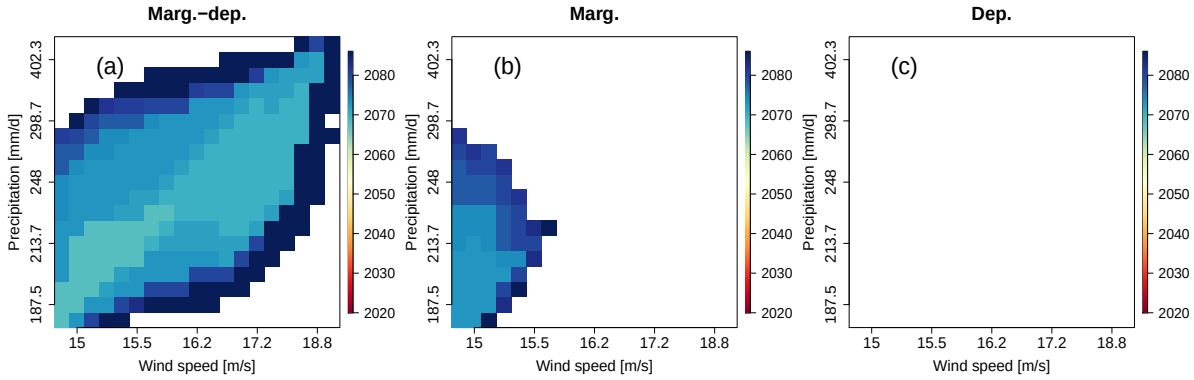

Figure S1. Same as Fig. 6 but for 95% confidence level: CNRM-CM6 (a-c) time of emergence at 95% confidence level for compound wind and precipitation extremes due to changes of (a) both marginal and dependence properties, (b) marginal properties only, and (c) dependence properties only. Results are presented for varying exceedance thresholds between the 5th and 95th percentile of compound wind and precipitation extremes data. White indicates that no time of emergence is detected.

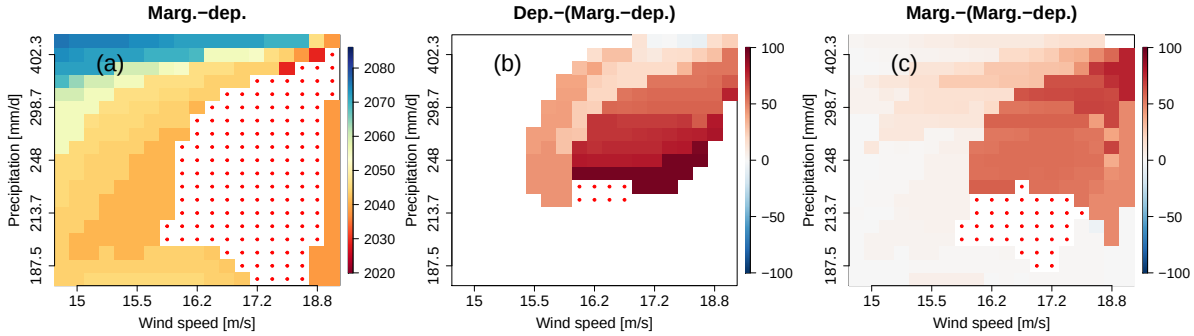

Figure S2. CNRM-CM6 differences of time of emergence at 68 % confidence level between time of emergence obtained by considering both marginal and dependence properties changes and (b) dependence properties changes only, and (c) marginal properties only. CNRM-CM6 (a) time of emergence at 68 % confidence level obtained by considering both marginal and dependence properties changes are also displayed. Color points indicate values lying outside the plotted ranges. White indicates that no time of emergence is detected.

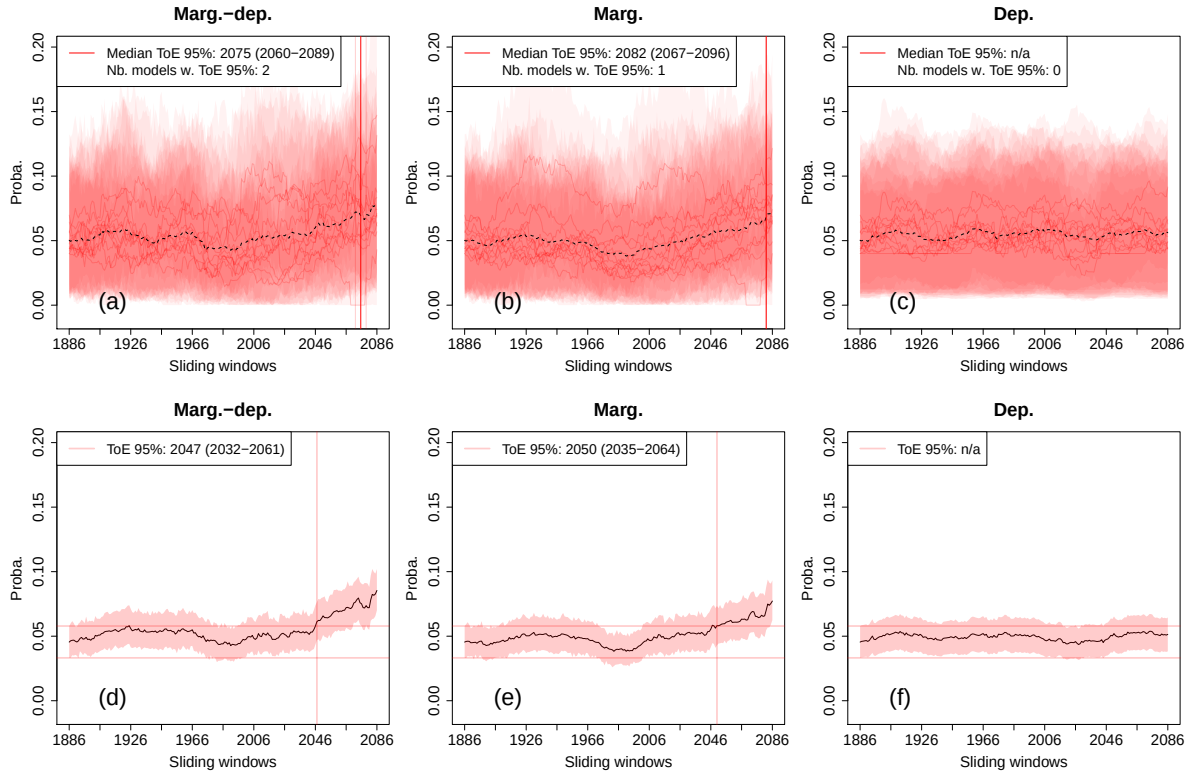

Figure S3. Same as Fig. 7 but for 95% confidence level: Probability changes and time of emergence (at 95%) of compound wind and precipitation extremes (exceeding the individual 80th percentiles of selected points of high values) for (a-c) Indiv- and (d-f) Full-Ensemble versions due to changes of (a,d) both marginal and dependence properties, (b,e) marginal properties only, and (c,f) dependence properties only. The shaded bands indicate 95% confidence intervals of the probabilities. For (a-c), individual time of emergence for the different models within the ensemble are displayed when defined (vertical light red lines), as well as the corresponding median time of emergence (vertical red lines). For information purpose, multi-model mean exceedance probability time series are also plotted (black dotted lines). Not-applicable (n/a) is indicated when no time of emergence is detected.

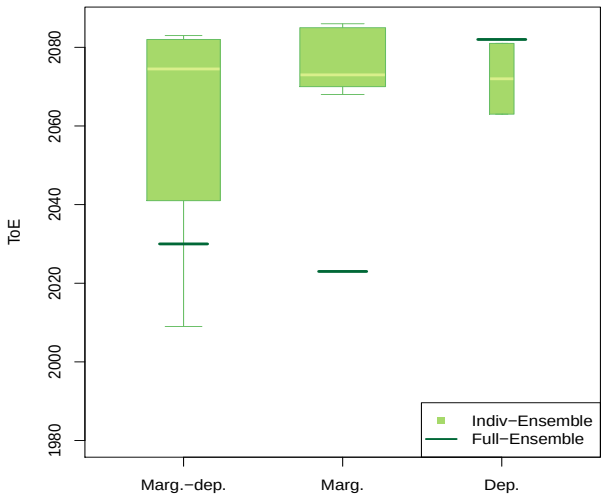

Figure S4. Boxplots of time of emergence at 68% confidence level of compound wind and precipitation extremes (exceeding the individual 80th percentiles of selected points of high values) for the Indiv-Ensemble version. Size of boxplots is proportional to the number of models presenting an emergence. For the Full-Ensemble version, values of ToE are indicated using lines.

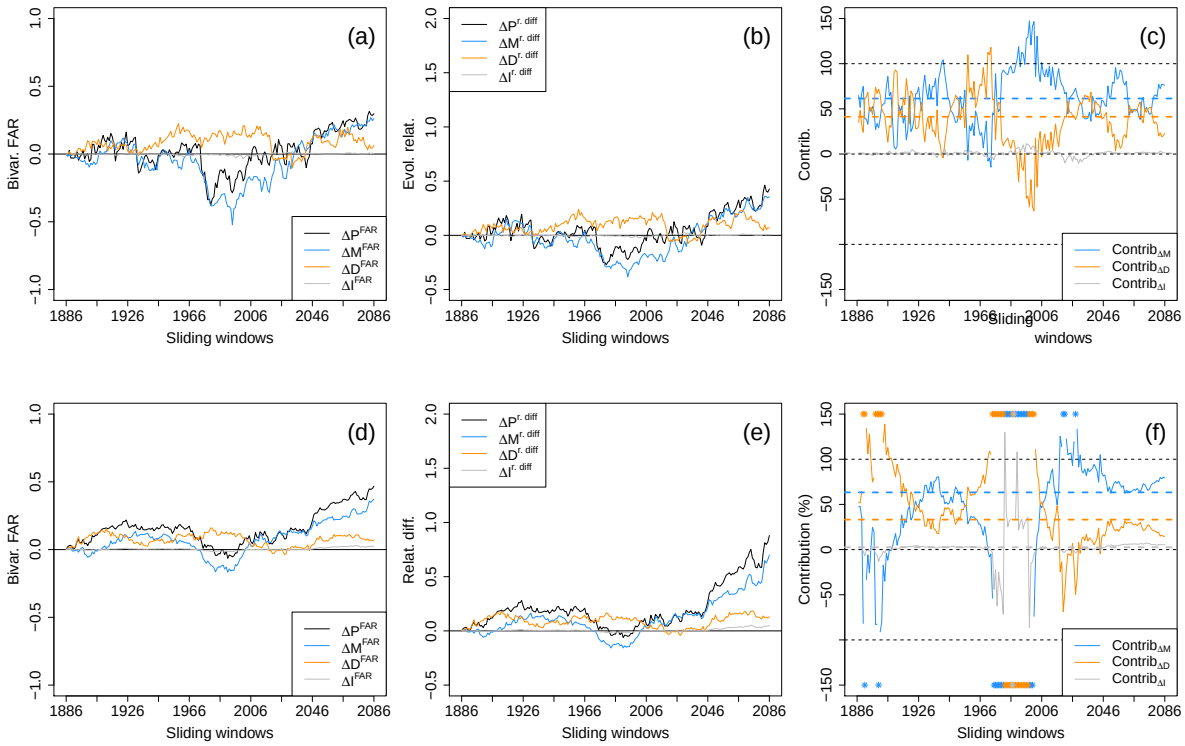

Figure S5. Evolutions of (a, d) the bivariate fraction of attributable risk (FAR), (b, e) relative difference of probabilities with respect to the reference period (1871-1900) and (c, f) contribution of the marginal, dependence and interaction terms to probability values for (a-c) Indiv- and (d-f) the Full-version. For the Indiv-Ensemble version (a-c), bivariate FAR, relative differences and contributions time series are computed by considering for each sliding window the median of the models' FAR, relative differences and contributions, respectively. Median contributions computed over all sliding windows are displayed with dotted lines. Asterisks indicate values lying outside the plotted range.

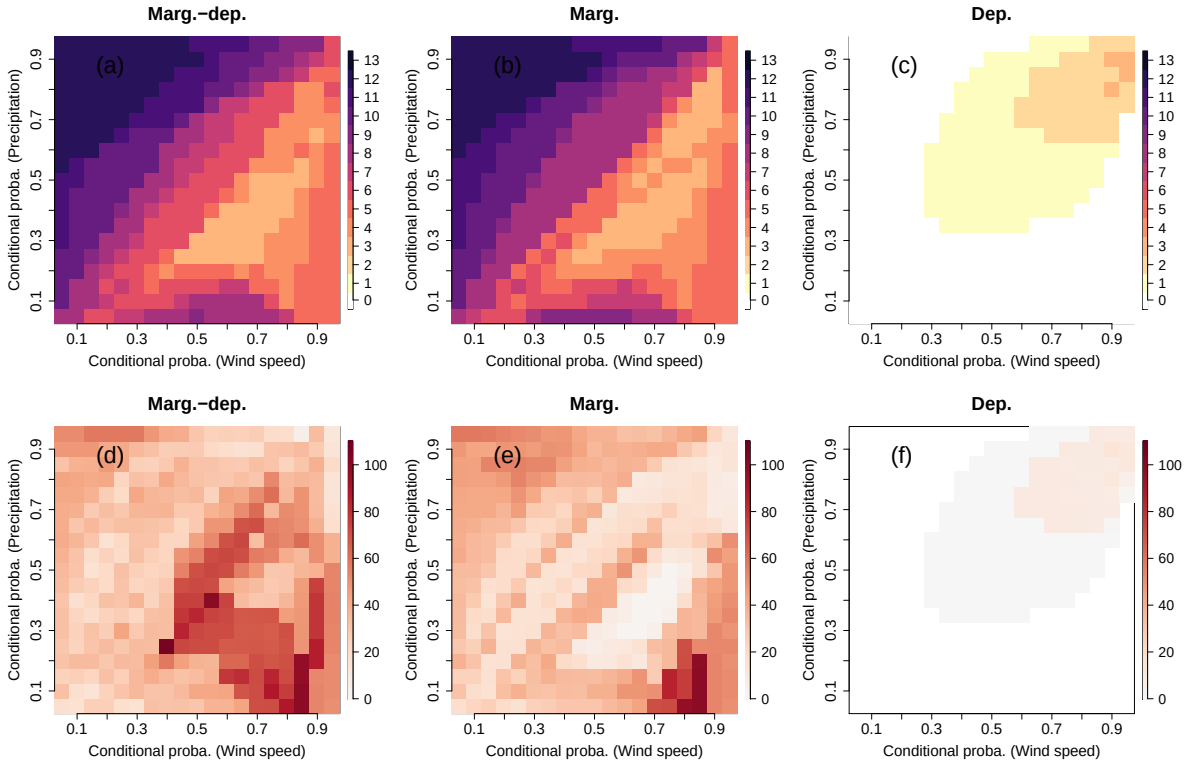

Figure S6. (a-c) Number of models within the Indiv-Ensemble framework presenting a time of emergence at 68% confidence level for compound wind and precipitation extremes. (d-f) Inter-quartile differences (Q3-Q1) of time of emergence.

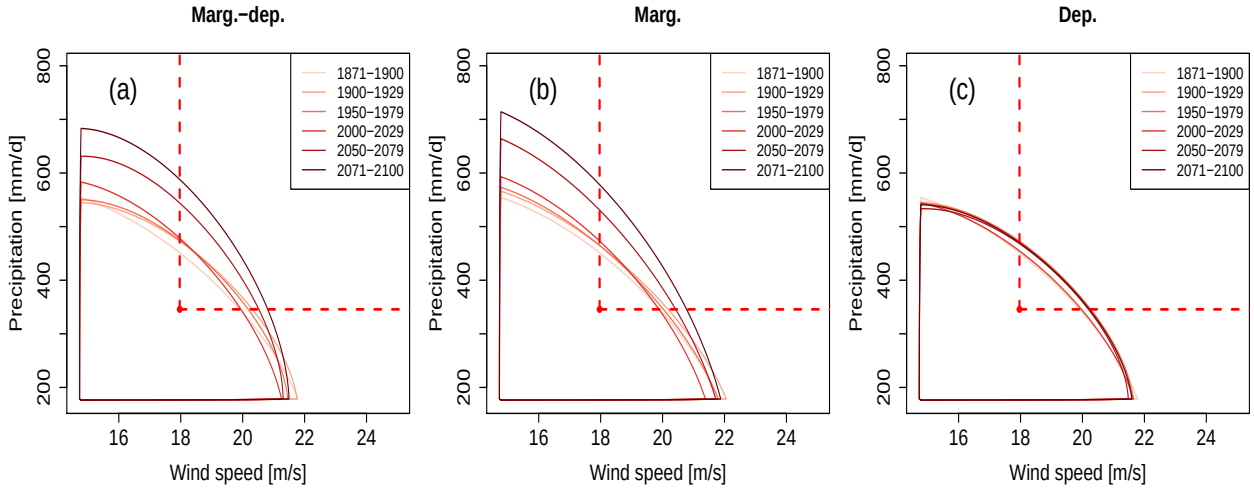

Figure S7. Same as Fig. 4 but for Full-Ensemble data: Change of compound wind and precipitation extremes distributions based on pooled data due to (a) marginal and dependence changes, (b) marginal changes while keeping dependence fixed and (c) dependence changes while keeping marginal fixed. For the bivariate distributions, contour lines encompassing 90 % of all data points are shown. A selection of six 30-years sliding windows is presented using a color gradient from light (1871-1900) to dark (2071-2100).

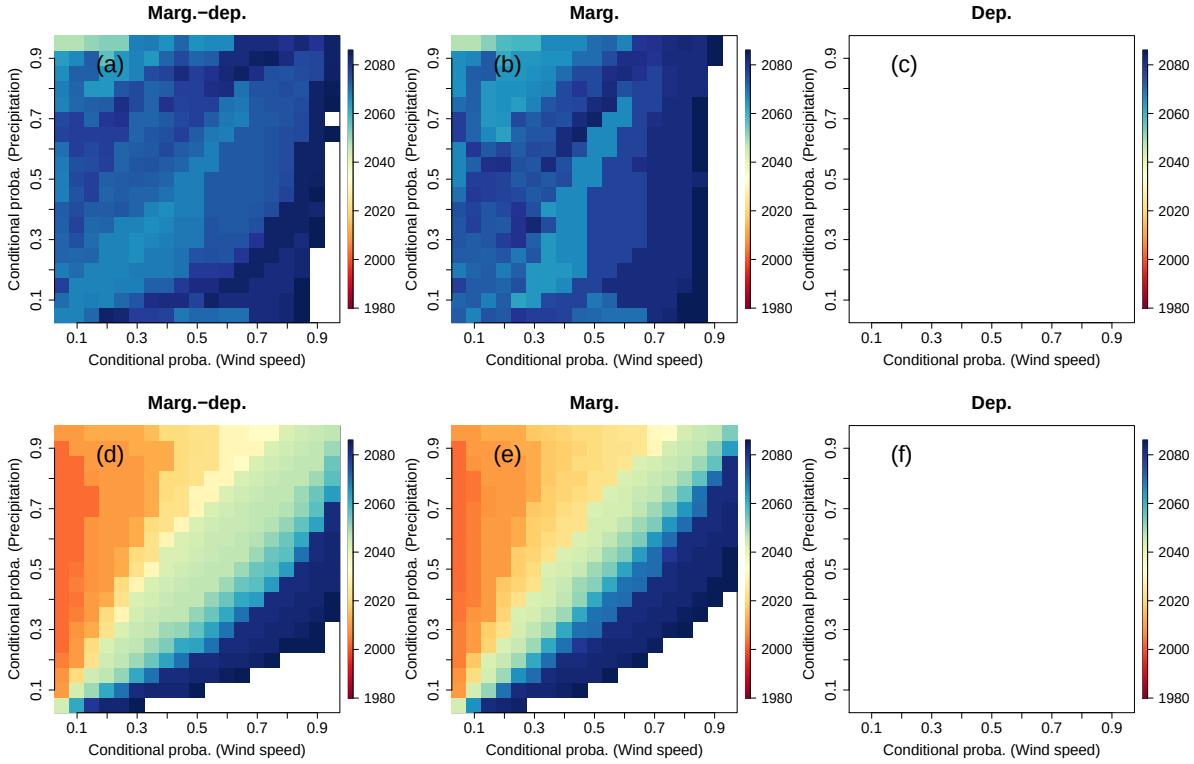

Figure S8. Same as Fig. 9 but for 95% confidence level: Time of Emergence (at 95% confidence level) matrices of compound wind and precipitation extremes due to changes of (a, d) both marginal and dependence properties, (b, e) marginal properties only, and (c, f) dependence properties only. Results are displayed for (a-c) the Indiv- and (d-f) Full-Ensemble versions for varying exceedance thresholds between the 5th and 95th percentile of compound wind and precipitation extremes data. For each subplot, white indicates that no time of emergence is detected.

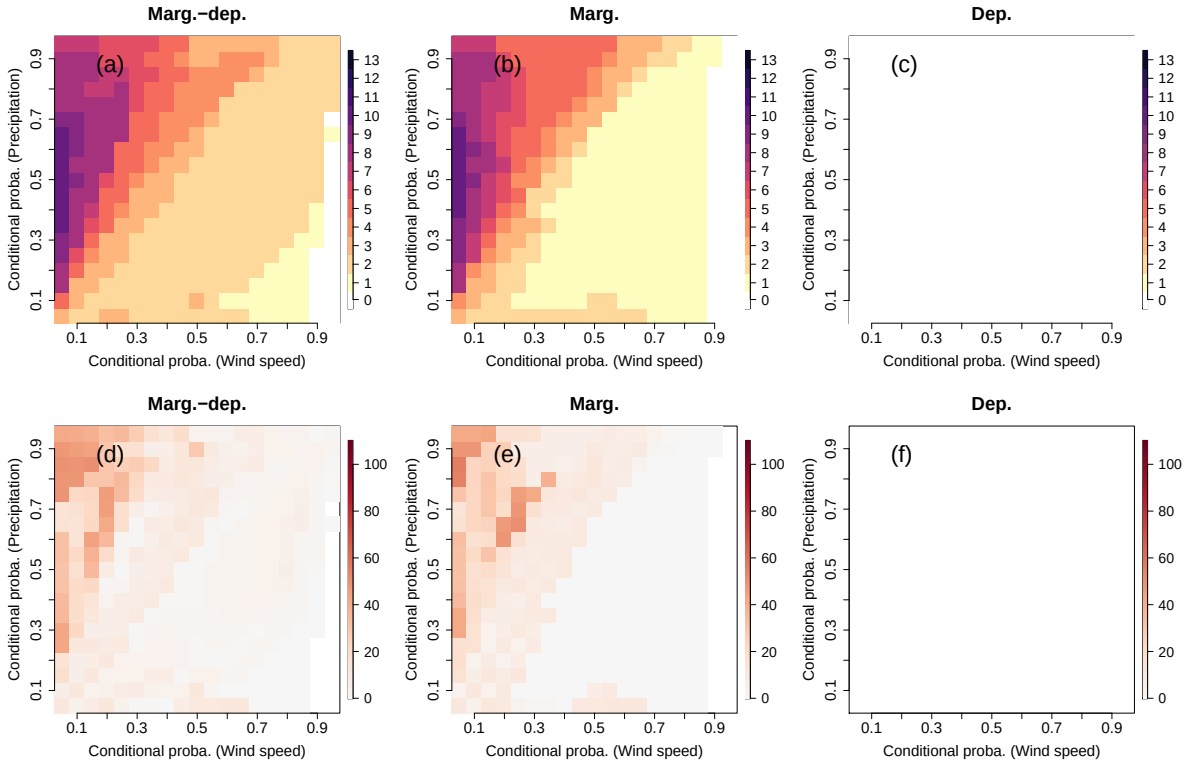

Figure S9. Same as Fig. S6 but for 95% confidence level: (a-c) Number of models within the Indiv-Ensemble framework presenting a time of emergence at 95% confidence level for compound wind and precipitation extremes. (d-f) Inter-quartile differences (Q3-Q1) of time of emergence.

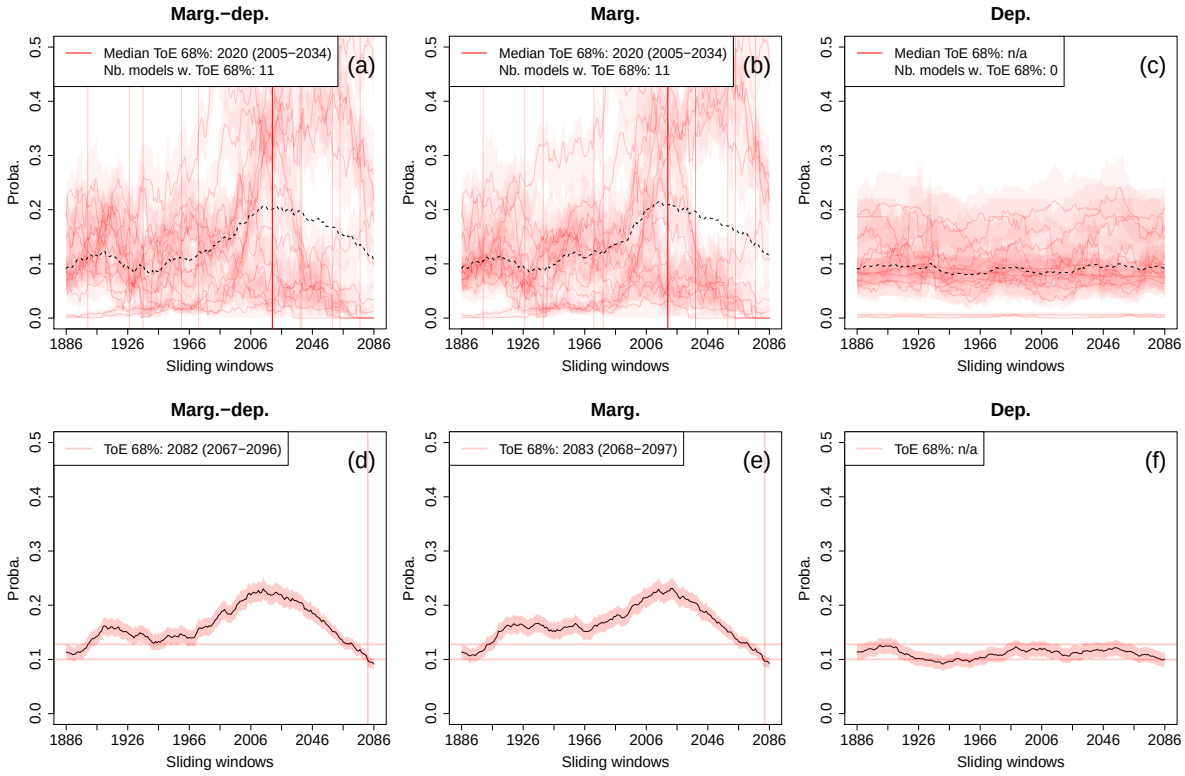

Figure S10. Same as Fig. 12 but for GDD $\geq$ 150 °C.d and minimal temperatures $\leq$ 0 °C: Probability changes and time of emergence (at 68%) of growing-period frosts (GDD $\geq$ 150 °C.d and minimal temperatures $\leq$ 0 °C) for (a-c) Indiv- and (d-f) Full-Ensemble versions due to changes of (a, d) both marginal and dependence properties, (b, e) marginal properties only, and (c, f) dependence properties only. The shaded bands indicate 68% confidence intervals of the probabilities. For (a-c), individual time of emergence for the different models within the ensemble are displayed when defined (vertical light red lines), as well as the corresponding median time of emergence (vertical red line). For information purpose, multi-model mean exceedance probability time series are also plotted (black dotted lines). Not-applicable (n/a) is indicated when no time of emergence is detected.

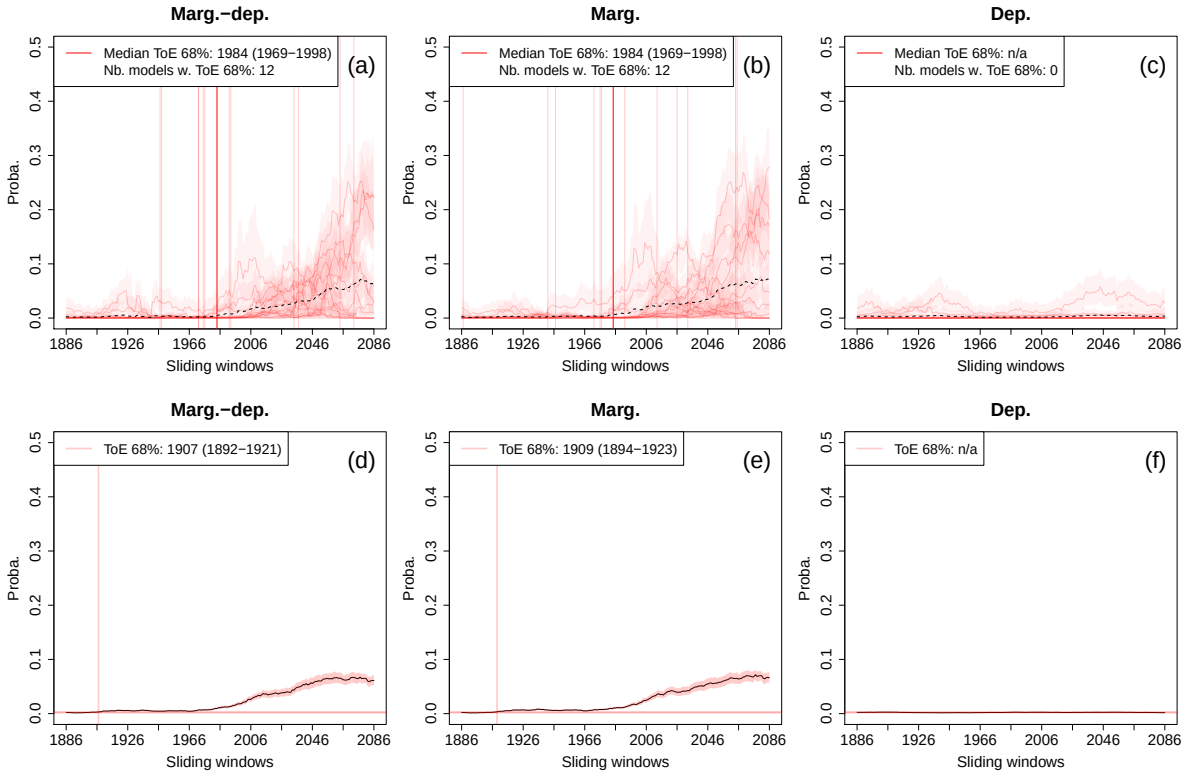

Figure S11. Same as Fig. 12 but for GDD $\geq$ 250 °C.d and minimal temperatures $\leq$ 0 °C: Probability changes and time of emergence (at 68%) of growing-period frosts (GDD $\geq$ 250 °C.d and minimal temperatures $\leq$ 0 °C) for (a-c) Indiv- and (d-f) Full-Ensemble versions due to changes of (a, d) both marginal and dependence properties, (b, e) marginal properties only, and (c, f) dependence properties only. The shaded bands indicate 68% confidence intervals of the probabilities. For (a-c), individual time of emergence for the different models within the ensemble are displayed when defined (vertical light red lines), as well as the corresponding median time of emergence (vertical red line). For information purpose, multi-model mean exceedance probability time series are also plotted (black dotted lines). Not-applicable (n/a) is indicated when no time of emergence is detected.

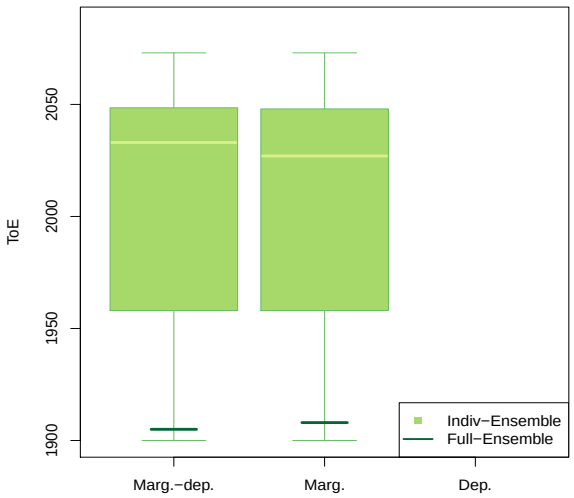

Figure S12. (a) Boxplots of time of emergence at 68% confidence level of growing-period frosts (GDD $\geq 200\ ^{\circ}$C.d and minimal temperatures $\leq 0\ ^{\circ}$C) for the Indiv-Ensemble version. Size of boxplots is proportional to the number of models presenting an emergence. For the Full-Ensemble version, values of ToE are indicated using lines.

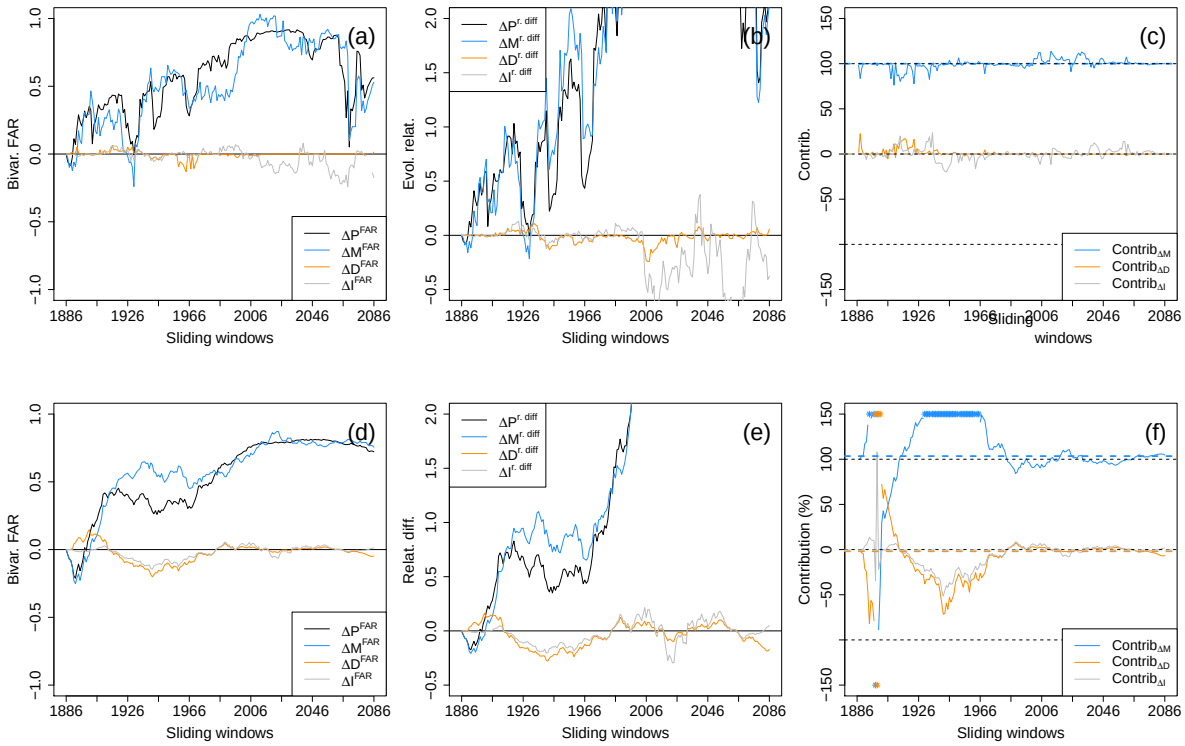

Figure S13. Same as Fig. S5 but for growing-period frost events ($GDD \geq 200 \cap T \leq 0$). Evolutions of (a, d) the bivariate fraction of attributable risk (FAR), (b, e) relative difference of probabilities with respect to the reference period (1871-1900) and (c, f) contribution of the marginal, dependence and interaction terms to probability values for (a-c) Indiv- and (d-f) the Full-version. For the Indiv-Ensemble version (a-c), bivariate FAR, relative differences and contributions time series are computed by considering for each sliding window the median of the models' FAR, relative differences and contributions, respectively. Median contributions computed over all sliding windows are displayed with dotted lines. Asterisks indicate values lying outside the plotted range.

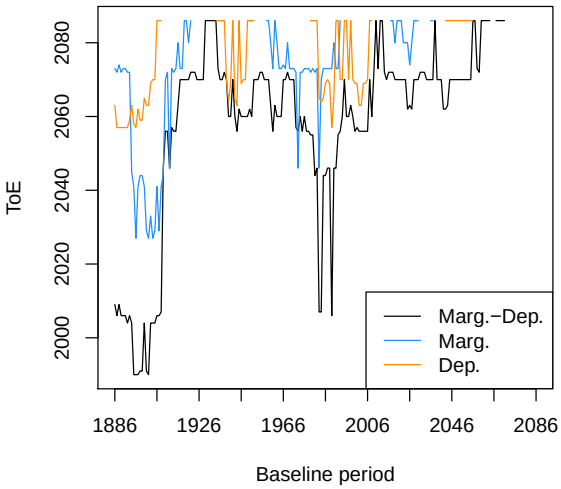

Figure S14. CNRM-CM6 time of emergence (at 68% confidence level) of compound wind and precipitation extremes probabilities ($\mathbb{P}(X > x_{80\text{lsel}} \cap Y > y_{80\text{lsel}} \mid (X,Y) \in S_{90,90}^{\text{CNRM-CM6}})$) for different baseline periods. Time of emergence are computed for probability time series when considering changes of both marginal and dependence properties ("Marg.-Dep."), marginal properties only ("Marg."), and dependence properties only ("Dep."). A blank space is left when no time of emergence is detected.